The effect of variant glucose and oxygen concentrations on the differentiation of humane mesenchymal stem cells (hMSC)

Bachelor's assignment

University of Twente

Biomedical Technology

Babet Roekevisch

DBE

30/11/2023

Supervisor: Janine Post

Daily supervisor: Jacqueline Plass

External member: Ruchi Bansal

Acknowledgement

I hereby present my bachelor's final assignment on the impact of glucose and oxygen on the differentiation of hMSCs. In this report, I investigated the effects of glucose and oxygen on the differentiation of hMSCs into chondrocytes, adipocytes and osteocytes, aiming to optimize the culture conditions for hMSCs.

First and foremost, I would like to express my gratitude to my daily supervisor, Jacqueline Plass. Her excellent guidance and willingness to dedicate her time to assist me with this assignment have been invaluable. Additionally, I extend my thanks to Janine Post, the chair of the graduation committee, for her responsiveness to my inquiries and her evaluation of my project. I also appreciate the participation of Ruchi Bansal as an external member of the committee, contributing to the assessment of my assignment.

I want to acknowledge Nicole Baars and all my fellow students who assisted me in brainstorming various aspects of the assignment. Finally, I would like to express my sincere appreciation to my family and friends for their unwavering support throughout this journey. Thank you!

Abstract

In this study, the impact of glucose and oxygen concentrations on the differentiation of hMSCs into chondrocytes, osteocytes and adipocytes is investigated. Glucose is a crucial molecule utilized in cellular energy production, while oxygen dictates whether this process occurs aerobically or anaerobically. By testing various conditions, the aim is to draw conclusions regarding the optimal conditions for differentiation into the different cell types. Cells were cultured for 21 days in both high (4.5 g/L) and low (1 g/L) glucose concentrations, under both normoxic (21% oxygen) and hypoxic (2.5% oxygen) conditions. After 21 days, cytochemical and immunohistochemical staining were conducted to draw conclusion about the most favorable conditions for differentiation. The study concludes that for chondrogenic differentiation, a high concentration of glucose and normoxic conditions yield the best results, as evidenced by significant Alcian Blue staining and the presence of COL2a. In adipogenic differentiation, no significant difference was observed between high and low glucose concentrations, but normoxia exhibited better adipogenic differentiation compared to hypoxia. For osteogenic differentiation, no conclusions can be drawn as the cells did not undergo differentiation.

Table of contents

List of abbreviations

Abbreviations	Meaning
ACAN	Aggrecan
Alpha-MEM	Alpha modification minimum essential medium
AMPK	AMP-activated kinase
ASAP	Apoptosis- and splicing-associated protein
ATP	Adenosine triphosphate
Beta-GP	Beta-glycerolphosphate
BFGF	Basic fibroblast growth factor
BMP2	Bone morphogenetic protein 2
CESC's	cervical squamous cell carcinoma
COL1	Collagen 1
COL2a	Collagen 2a
COL 10	Collagen 10
CTA	Citric tricarboxylic acid
dH_2O	Distilled water
DKK1	Dickkopf-1
DMEM	Dulbecco's Modified Eagle Medium
FBS	Fetal bovine serum
GREM1	Gremlin 1
HCl	Hydrochloric acid
HG	High glucose
HIF1a	Hypoxia inducible factor 1 subunit alpha
HIF2a	Hypoxia inducible factor 2 subunit alpha
hMSCs	Human mesenchymal stemcells
H_2O_2	Hydrogenperoxide
LG	Low glucose
MMP13	Matrix Metalloproteinase-13
OKC	odontogenic keratocyst
PANX3	Pannexin 3
PBS	Phosphate buffered saline
Pen/strep	Penicillin/Streptomycin
PKC	Protein kinase C
PPAR-gamma	Peroxisome proliferator-activated receptor gamma
ROS	Reactive oxygen species
Sod.pyr	Sodium pyruvate
SOX9	SRY-Box Transcription Factor 9
TGF-β	Transforming growth factor β
TGF-βRII	Transforming growth factor β receptor 2

H1 Introduction

Cell culture is a fundamental technique in modern research. It allows scientists to study cellular behavior, molecular mechanisms and various physiological processes. For a viable cell culture, sterile technique, precise nutrient composition and optimal environmental conditions are required. In this paper, our focus revolves around optimizing the differentiation of human mesenchymal stem cells (hMSCs), by researching the influence of glucose and oxygen concentrations.

hMSCs represent a category of undifferentiated cells with numerous advantageous traits. These cells exhibit robust proliferation (self-renewal) capabilities, possess the ability to differentiate into various cell types and tissues, and can be readily obtained. Classified as multipotent cells, hMSCs have the capacity to differentiate into tissues derived from a single germ layer, specifically the mesoderm layer. Consequently hMSCs are capable of differentiation into mesoderm-derived tissues, including cartilage, bone and adipose tissue (5).

To differentiate hMSCs into the appropriate cell lineage, specific proteins must be added to the differentiation medium, as outlined in section 2.2. Operating under the assumption that the body represents the optimal cultivation environment, researchers aim to mimic these conditions in in vitro cell culture. In recent times, there has been a growing awareness among scientist regarding the impact of culture conditions on cell cultures, leading to increased research into the optimal conditions for cell cultivation.

Currently, hMSCs are often cultured in a medium based on alpha-MEM. Alpha-MEM contains a glucose concentration of 1 g/L, considered low in this study. However, when hMSCs undergo differentiation into chondrocytes or adipocytes, the alpha-MEM is replaced with DMEM, which contains 4.5 g/L glucose (considered high in this study). But when differentiated into osteocytes, alpha-MEM continues to be used (6). Glucose plays a significant role in cellular processes as an energy source and has an influence on different signal pathways. Determining the in vivo glucose concentration in a specific cell-type is challenging due to various factors such as vascularity and dietary habits, but is around 110 mg/dL in non-diabetics (7). Which is much lower than the glucose concentration in DMEM. Therefore, it becomes intriguing to investigate which glucose concentration leads to the best differentiation. Additionally, cells are cultured in a 21% oxygen concentration, reflecting the standard oxygen concentration on earth. However, examination of in vivo conditions reveals that nowhere in the body is the oxygen concentration 21% (8). From the standpoint that in vivo represents the optimal culture conditions, scientists are now exploring the influence of oxygen concentration on hMSCs cultivation and differentiation.

This leads to the aim of this study, which is to investigate the influence of high and low concentrations of glucose and oxygen on the differentiation of hMSCs into chondrocytes, adipocytes and osteocytes. This is done through cell culture, where human stem cells from two donors are cultured from the femur. The stem cells are then pooled and divided into the three different differentiation lines. For each differentiation line, two differentiation media are used, one with high glucose concentration (4.5 g/L) (HG) and one with low glucose concentration (1 g/L) (LG). Additionally, this experiment is performed in both normoxia and hypoxia conditions. Using cytochemical staining and immunohistochemistry (for staining metabolisms see appendix A and B), the conditions are tested to assess the extent of differentiation. Hopefully, this will provide answers to draw conclusions about which condition is optimal for the differentiation of hMSC's.

H2 Background information

H2.1 Glucose influence

Glucose is one of the main nutrients of the cell. It can be transported into the cell by various enzymes, such as GLUT1, GLUT3 and GLUT 4 (9). Glucose produces ATP through glycolysis, giving the cell energy to grow, differentiate and do other cellular metabolisms. When culturing cells in normoxia, glucose is converted into pyruvate through glycolysis. Through this process one glucose molecule is converted into two pyruvate molecules. The pyruvate (3C) is then converted into Acetyl-COA (2C). This delivers one NADH molecule. The acetyl-COA can then be converted by the citric acid cycle (CTA), resulting in 36 ATP molecules. For a better explanation about the CTA, see appendix C. When a cell experiences insufficient glucose availability, the cell shifts to utilizing amino acids exclusively for cellular catabolism to address the glucose deficit. Research has indicated that this transition occurs after reaching a concentration of 0,54 mmol/L. This underscores that a glucose deficit can impact cell growth and proliferation (10). What the influence of different glucose concentration is for the different cell lines will be discussed in the subchapters below.

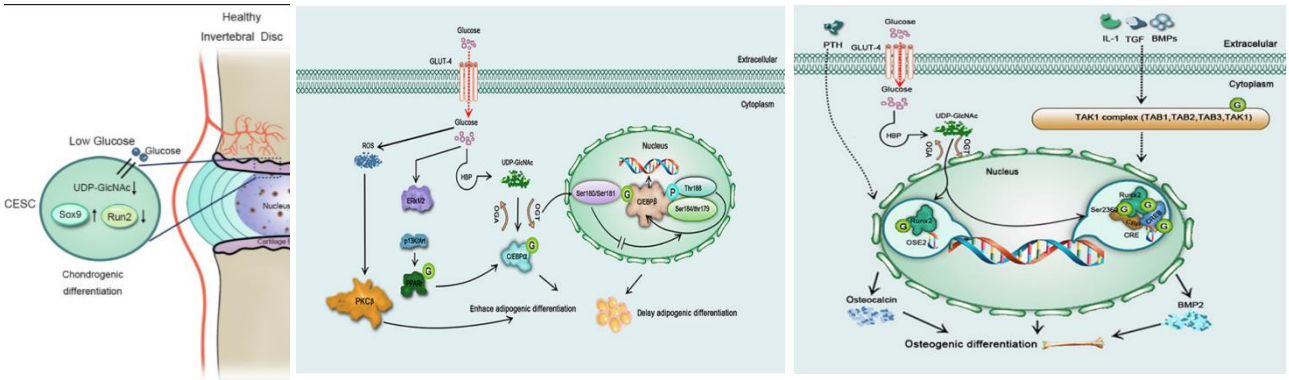

Figure 1, Describes the impact of glucose on various cell types. On the left, the influence of glucose on chondrocytes is elucidated. As depicted in the figure, low glucose concentration affect the transcription factors SOX9 and RUNX2. The figure illustrates a positive impact on SOX9 and a negative impact on RUNX2 (2). In the middle panel, the effect of glucose on adipogenesis is presented. As shown in the figure, glucose stimulates dipogenic differentiation through positive modulation of the ROS complex and PKC complex (3). The right panel depicts the influence of glucose on osteocytes. As observed in the panel, osteogenic differentiation is promoted through positive modulation of RUNX2, BMP2 and osteocalcin (3).

H2.2 Oxygen influence

This research also addresses the impact of normoxia and hypoxia on the differentiation of hMSCs. Recent research suggest a potential link between the fate determination of hMSCs and the oxygen concentration in their microenvironment. As we investigate the influence of glucose and oxygen, four conditions are established for cultivation: high glucose concentration in both normoxia and hypoxia, as well as low glucose concentration in normoxia and hypoxia. In hypoxic conditions, the conversion of pyruvate to lactate occurs, yielding only 2 ATP molecules instead of 36 ATP molecules (11). This implies that when cells are cultured in hypoxia, less energy is generated compared to cells cultured in normoxia. Consequently, cellular processes tend to operate at a slower pace. In general, hypoxia results in reduced cellular energy availability, and a low glucose concentration further limits the energy resources accessible to the cells. Besides the influence of hypoxia on the energy metabolism, hypoxia also influences some signal pathways. This is discussed in the next subchapters.

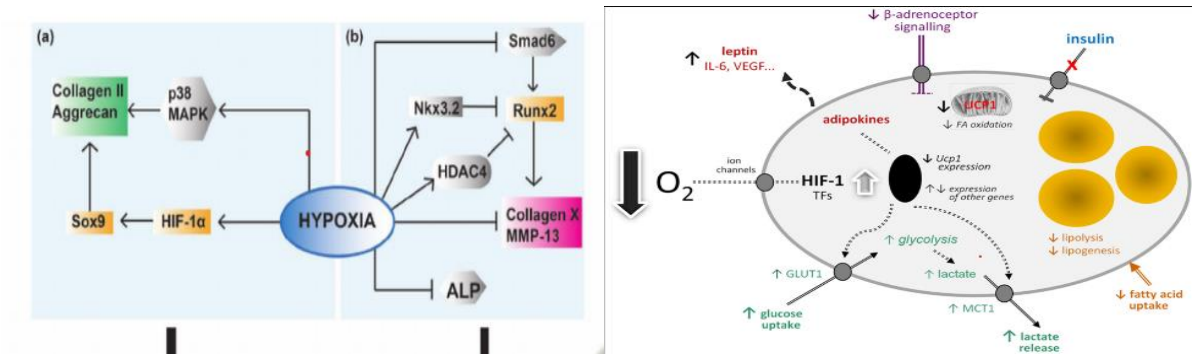

Figure 2, Left the influence of hypoxia on chondrogenic and osteogenic differentiation. Hypoxia has a positive effect on chondrogenic differentiation by stimulating COL2, SOX9 and aggrecan. While, on osteogenic differentiation, hypoxia inhibits RUNX2, MMP13 and COL10 (1). Right, the influence of hypoxia on adipogenic differentiation. Hypoxia stimulates a reduction in lipogenesis, resulting in less lipid droplets (4).

H2.3 Impact on chondrogenesis

Cartilage is avascular, meaning that cells do not have a rapid supply of glucose and the glucose molecules must enter the cells through capillaries of the epiphyseal artery via diffusion. This process is facilitated by GLUTs. While the influence of glucose on the hypertrophic state of chondrocytes differentiated from hMSCs is not entirely clear, research has explored the impact of glucose on CESC's. This study indicate that high glucose concentrations lead to an increase of COL1 and a decrease of COL2. Additionally, SOX9 is reduced, while RUNX2 is increased, which is seen figure 1. This implies that high glucose concentrations diminishes differentiation into cartilage and enhances differentiation into osteoblasts (2, 3).

Furthermore, research demonstrates that pre-culturing hMSCs in high glucose inhibits differentiation into chondrocytes. Growing cells in high glucose suppresses OKC activity, subsequently impacting TGFβRII, which is inhibited. The inhibition of TGFβRII results in the inhibition of TGF-β, leading to the suppression of chondrogenesis. For optimal chondrogenic culture, hMSCs should be cultured in low glucose (12).

In chondrogenesis differentiation, normoxia has been shown to stimulate the production of late hypertrophic chondrocyte differentiation markers, including MMP13, PANX3 and collagen X, seen in figure 2. These markers are associated with the ossification of chondrocytes (13, 14). Conversely, hypoxia conditions induce the production of SOX9, COL2a, ACAN, GREM1, FRZB and DKK1, which are inhibitors of hypertrophic differentiation (14). Meaning that hypoxia can stimulate chondrogenic differentiation, while normoxia stimulates osteogenic markers (8).

H2.4 Impact on adipogenesis

In adipogenesis, ROS and PKC play pivotal roles and both processes are amplified by elevated glucose concentrations, contributing to a stimulation of adipogenesis, seen in figure 1. Furthermore, high glucose levels enhance lipid formation in adipogenesis through the PPAR-gamma signaling pathway (3, 15). Meaning that glucose has a positive effect on adipogenic differentiation.

Hypoxia negatively affects the formation of PPAR-gamma, a crucial protein for stimulating adipogenesis differentiation. The expression of PPAR-gamma is inhibited due to acetylation of histones H3 and H4. Additionally, hypoxia influences the activation of AMP-activated kinase (AMPK). Research has shown that AMPK stimulation has a unfavorable effect on adipogenesis. Also, hypoxia inhibits the lipogenesis process, resulting in less lipid droplets, seen in figure 2. Moreover, AMPK inhibits clonal expansion, leading to a suppression of adipocytes (16).

H2.5 Impact on osteogenesis

When considering osteogenesis, a high glucose concentration has a positive influence on the differentiation of hMSCs into osteocytes. In addition to the TCA cycle, glucose can also be utilized for the production of the hexosamine pathway. Through this pathway, glucose exerts a positive influence on RUNX2, a key regulator of osteogenic gene expression, thereby promoting osteogenic differentiation (17).

Furthermore, research has demonstrated that an excessively high glucose concentration diminish osteogenesis. An optimum concentration of 15.5 mM has been identified. This concentration leads to an increase in proliferation, mineralization, osteogenic genes, such as RUNX2 and osterix, and BMP2, see figure 1. These transcription factors are upregulated due to the generation of reactive oxygen species (ROS), which positively influences their production. However, an excessively high glucose concentration results in an exaggerated ROS level, ultimately inhibiting osteogenesis through the activation of the AKT pathway (3, 18).

Hypoxia significantly influences hMSCs differentiation into osteocytes. Low oxygen conditions activate HIF1A, which, in turn, stimulates SOX9, inhibiting SP7 and suppressing osteoblast differentiation. HIF1A also inhibits RUNX2, a critical protein in osteoblast matrix formation, see figure 2. Furthermore, hypoxia affect the wnt-signaling pathway by inducing the production of sclerostin. In the context of osteoclast differentiation, hypoxia exhibits a positive feedback loop by stimulating HIF2A, which promotes osteoclastogenesis. Both HIF1A and HIF2A positively influence the expression of resorptive genes, indicating the initialization of osteoclast formation. Resulting in a down regulation of osteocytes (19, 20).

Based on this information, I formulate my hypothesis. I anticipate that elevated glucose concentration will have a detrimental effect on chondrogenic differentiation, leading to hypertrophy in chondrocytes. Additionally, I expect HG to exert a positive influence on the differentiation of adipocytes and osteocytes by stimulation cell specific genes. Moreover, I hypothesize that hypoxia will positively impact chondrogenic differentiation by inhibiting hypertrophic proteins. Conversely, I anticipate that hypoxia will have a negative effect on adipocytes and osteocytes by suppressing cell-specific genes.

H3 Material and methods

H3.1 Cell culture

Donor D42 and D56 hMSCs vials from passage 2 were defrosted from nitrogen and each vial was plated into two 175 mL flask, for both normoxia and hypoxia. The hMSCs were cultured in a proliferation medium containing α-MEM (Invitrogen, 41965-062) enriched with 10% v/v FBS (sigma, F7524), 100 U/mL pen/strep (Invitrogen, 15140-163), 2mM glutaMAX (Invitrogen, 35050-087), 50 µg/mL AsAP (sigma, A8960-5G) and 1 ng/µL bFGF (neuromics, PR80001-50) and incubated in a humidified incubator at 37 degrees in normoxia and hypoxia (XVIVO). Every 3-4 days the proliferation medium was refreshed and hMSC's were observed with the EVOS microscope. When 80% confluency was reached, cells were washed with PBS (Invitrogen) and detached using 0.25% v/v trypsin/EDTA (Invitrogen, 25200-072).

H3.2 Multilineage differentiation

Cells were seeded into one 96-wells plate (Greiner, 650-185)(200.000 cells/well chondrogenic differentiation), one 12-wells plate (Greiner, 665-180)(50.000 cells/well adipogenic differentiation) and one 12-wells plate (Greiner)(4.000 cells/well osteogenic differentiation). Cells were cultured for 3 weeks.

For chondrogenic differentiation, cells were cultured in 3D in a 1) high glucose differentiation medium containing DMEM (Invitrogen, 41965-062), supplemented with 100 U/mL pen/strep (Invitrogen, 15140-163), 50 mg/mL ITS-premix (Invitrogen, 41400-045), 40 µg/mL proline (Sigma, P5607-25G), 50 µg/mL AsAP (Sigma, A8960-5G), 100 mM sod. Pyr (Sigma, S8636), 10 ng/mL TGFbeta3 (R&D system, 243-B3-200) and 10-7 M dex (Sigma, D8893). 2) low glucose differentiation medium, DMEM (Invitrogen, 11885) and all the other supplements named above were used, except sod.pyr.

Also for adipogenic differentiation, cells were cultured in 2D in a 1) high glucose differentiation medium containing DMEM (Invitrogen, 41965-062), supplemented with 10% v/v FBS (Sigma, F7524), 100 U/mL pen/strep (Invitrogen, 15140-163), 2mM glutaMAX (Invitrogen, 35050-087), 10-6 M dex (Sigma, D8893), 10 µg/mL insulin (Sigma, I9278), 0,5 mM IBMX (Sigma, I5879), 0,2 mM indomethacin (Sigma, 57413) and 100 mM sod. Pyr. (sigma, s8636). 2) low glucose differentiation medium containing DMEM (Invitrogen, 11885) and all the other supplements named above, except sod.pyr.

At last, for osteogenic differentiation cells were cultured in 2D in a 1) Low glucose differentiation medium using α-MEM (Invitrogen, 41965-062), supplemented with 10% v/v FBS (Sigma, F7524), 100 U/mL pen/strep (Invitrogen, 15140-163), 2mM glutaMAX (Invitrogen, 35050-087), 50µg/mL AsAP (Sigma, A8969-5G), 0,01 M beta-GP (Sigma, 50020) and 10-8 M dex (Sigma, D8893). 2) high glucose differentiation medium using α-MEM (Invitrogen, 41965-062) enriching it with 3.5 g/L glucose (Gibco, 15023-021) and adding all the other supplements named above.

Every 3-4 days, differentiation medium was refreshed and cells were observed using a EVOS microscope.

H3.3 Pellet width measurement

Pellet size measurements are conducted over a 21-day period, specifically on day 7, 14 and 21, utilizing the ImageJ software. Three pellets from each experimental condition are measured, and these values are averaged and plotted. This analysis allows for the assessment of pellet growth or shrinkage over time. These size dynamics serve as an additional rationale to evaluate the effectiveness of pellet differentiation, providing insight into the comparative performance of the various experimental conditions.

H3.4 Cytochemical staining

For Alcian Blue, Pellets were fixated for 1 hour using 10% buffered formalin, dehydrated and embedded in paraffin using standard protocol. Paraffin embedded pellets were cut at 5 µm, dried at 37 degrees overnight rehydrated and stained with Alcian Blue (0.5% v/v, in H_2O, pH=1 adjusted in HCl). After rinsing with water, slides were counterstained with nuclear fast red (0.1% v/v in 0.5% v/v aluminum sulfate), washed with

water again, dehydrated and mounted. Data of stained slides is obtained by an Hamamatsu Nanozoomer. The data is been scored on a scale from 0 to 5, whereby 0 means no visible blue staining and 5 the most visible blue staining within the four conditions. This scoring system was applied to evaluate intensity, fibroblast-like structure and centered differentiation of the staining. Positive values were assigned to the intensity and centered differentiation scores, reflecting their desirability in a chondrocyte pellet. In contrast, a negative value was attributed to the fibroblast-like structure score, as it is considered unfavorable in the context of a chondrocyte pellet. Cumulative scores were obtained by summing these values. The pellet condition with the highest cumulative score is regarded as the most chondrocyte-like structure, while the pellet condition with the lowest cumulative score is deemed the least favorable.

Oil red O staining was performed in 12 wells-plate, on monolayer cells. Cells were fixated with 10% v/v buffered formalin, rinsed with PBS (Invitrogen) and stored at 4 degrees overnight. Cells were washed with dH_2O, incubated in 60% v/v isopropanol (diluted with dH_2O), stained with freshly filtered oil-red-o solution and washed with dH_2O. Images were acquired with a Nikon eclipse TE 300. For quantification, wells are washed again with dH_2O and 60% v/v isopropanol to remove aspecific staining. The remaining stain is extracted by adding 4% v/v Nonidet P-40, incubated for 15 minutes at a shaker and centrifuged. The absorbance of the supernatant of each condition is measured in triplicate at 540 nanometers.

And alizarin red S was performed on monolayer cells in 12 wells-plate. Cells were fixated with 10% v/v buffered formalin, rinsed with PBS (Invitrogen) and stored at 4 degrees overnight. Cells were washed with dH_2O, stained with freshly filtered Alizarin red S solution (pH 4.2) and again washed with dH_2O. Images were acquired with a Nikon eclipse TE 300.

H3.5 Collagen 2A IHC

Pellets were dried for 1 hour at 37 degrees, rehydrated, washed in dH_2O and placed in a sequenza working station. Antigen retrieval was done by using 0.1% g/v pepsine (Sigma P7000). After antigen retrieval pellets were washed with 0.1% v/v PBST and blocked with 0.3% v/v H_2O_2-PBS. Then pellets are washed again with PBS and blocked with 5% v/v BSA-PBS overnight at 4 degrees. Wash pellets with 0.1% v/v PBST and apply COL2a antibodies coupled to HRP diluted in 5% v/v BSA-PBS. Rinse the pellets with PBS and apply DAB-substrate solution. Wash pellets with dH_2O and counterstain with hematoxylin. Rinse the aspecific staining with running tap water and dehydrate the pellets. Cover the pellets with mounting medium and a coverslip. Images can be acquired using the Hamamatsu Nanozoomer.

H4 Results

H4.1 High glucose stimulates chondrogenic features

Over the course of a 21-day chondrogenic differentiation, we observed that pellets exhibited the most substantial growth in size under HG and normoxic conditions, as seen in figure 3. Notably, this growth is contingent on oxygen levels, with normoxia demonstrating greater expansion than hypoxia, as summarized in figure 4 illustrating the average pellet width over time.

Examining the HG normoxia condition, we observed an increase in pellet size at day 21, although a preceding decrease occurred until day 14. Conversely, no growth in other conditions pellet width was measured. However, it is noteworthy that the pellets in this conditions displayed less decrease between day 14 and day 21 compared to day 7 and day 14. Despite starting with the highest average pellet width, the hypoxia LG condition concluded with the smallest average pellet width, indicating the most pronounced decrease.

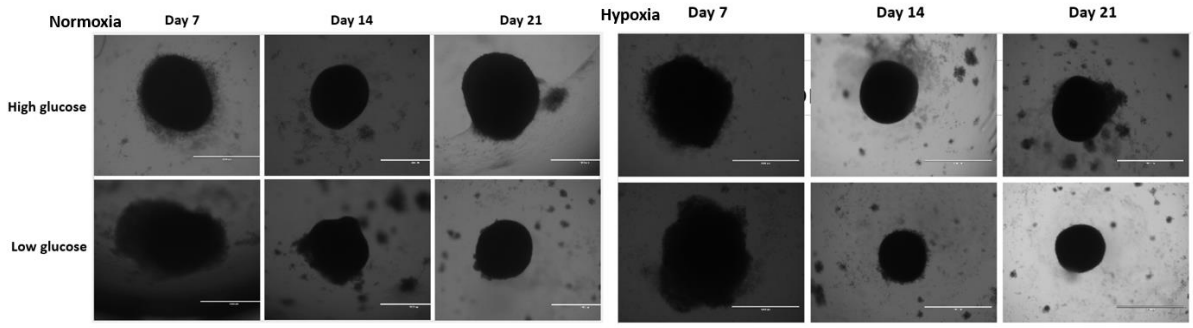

Figure 3, Chondrogenic differentiation was assessed through images captured the by EVOS microscope on days 7, 14 and 21 (scalebar is 1000 µm). In normoxic conditions (left), HG pellets exhibited a reduction in size on day 14 compared to day 7, followed by an increase in size by day 21. LG pellets transitioned from an initially voluminous and diffuse morphology to a compact structure. In hypoxic conditions (right), pellets similarly experienced a reduction in size, transitioning from a fluffy to a compact structure. Notable, there was no observed increase in pellet size under hypoxic conditions.

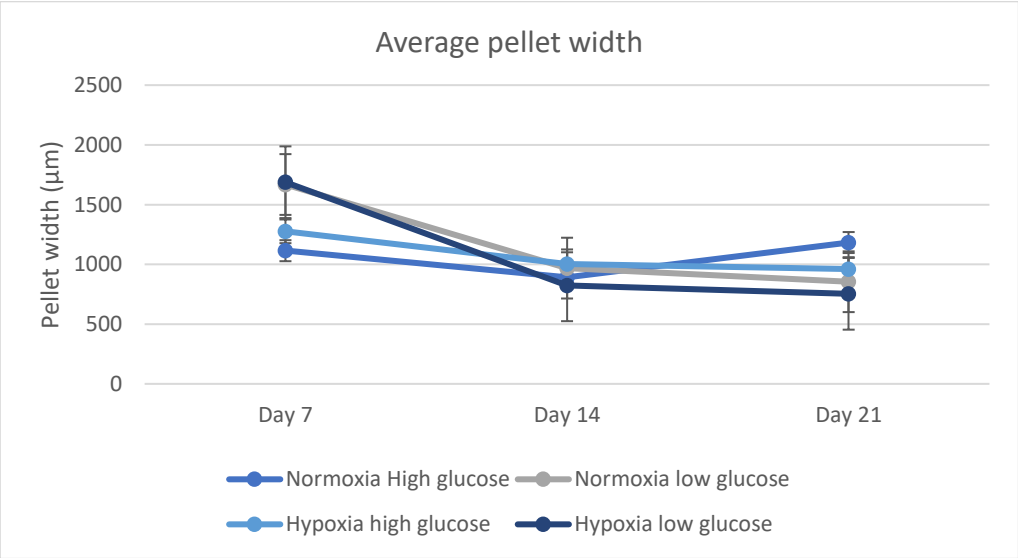

Figure 4, Analysis of chondrogenic pellet sizes was conducted for all four conditions at day 7, 14 and 21. In the case of HG normoxia, a reduction in pellet size is observed until day 14, followed by an increase at day 21. Conversely, the other conditions consistently exhibit a decrease in pellet size over time. Notably, LG hypoxia initially had the largest size at day 7 but eventually became the smallest, indicating the most significant reduction in pellet size.

Beyond pellet width, the shape of the pellets is an intriguing feature. At day 7 of differentiation, HG conditions exhibited a more compact and slightly more spherical structure compared to LG conditions, see figure 3. However, by the end of the three-week differentiation period (day 21), these differences in shape were no longer visible, as all conditions developed a spherical-like structure.

The superior chondrogenic differentiation in HG pellets was further validated through Alcian Blue staining. As illustrated in figure 5. HG pellets exhibited more Alcian Blue staining compared to those cultured in LG conditions. With more Alcian blue staining in normoxia compared to hypoxia.

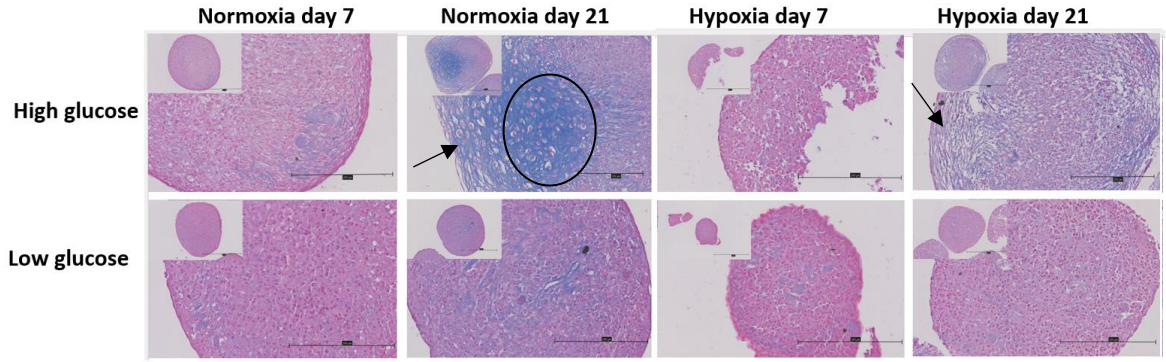

Figure 5, Alcian Blue staining was performed on chondrogenic pellets under different conditions: HG and LG in both normoxia and hypoxia. Pellet zoomed in has a scale bar of 250 µm and pellet zoomed out has a scale bar of 500 µm. At day 7, faint staining was observed in the pellets. However, by day 21, a pronounced blue staining was evident in the HG normoxia condition. Similarly, staining was observed in the HG hypoxia condition, but to a lesser extent. In contrast, staining the LG conditions was very weak, with a slightly more presence in LG normoxia than LG hypoxoia. Circle marks chondrocyte-like structure and arrows show fibroblastic structure.

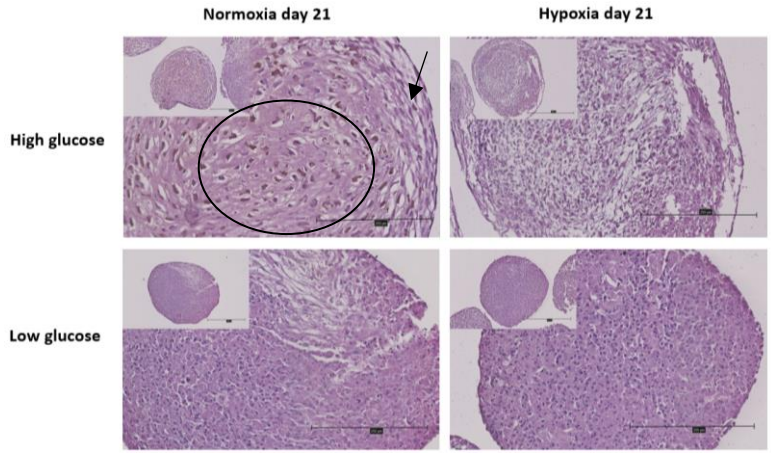

Figure 6, IHC of COL2a on chondrogenic pellets reveals the absence of COL2a in all conditions, except for HG normoxia. Zoomed in pellet has a scalebar of 250 µm and pellet zoomed out has a scalebar of 400µm. In HG normoxia, COL2a is exclusively localized in the chondrocyte-like structures (marked with a circle) and is not detected in the fibroblast-like structures (marked with an arrow).

In addition to the heightened Alcian Blue staining observed in HG pellets, there is a notable presence of chondrocyte-like structures in the HG normoxia condition. These structures are characterized by the presence of chondrocytes enclosed within chondrons surround by a substantial cell matrix, as depicted in figure 5 marked with a circle. Conversely, the HG hypoxia condition, despite displaying significant blue staining, lack chondrocyte-like structures. This condition present a looser arrangement and less desirable overall structure compared to the normoxia condition, marked with a arrow in figure 5 and 6. While LG pellets exhibit considerable less Alcian Blue staining than HG pellets, they display a markedly compact structure, despite this compactness, it does not manifest as a chondrocyte-like structure.

Table 1 presents the results of the Alcian blue pellet scoring, concluding that none of the conditions exhibit a truly chondrogenic-like structure as the highest total score is a 2,17 out of 5. It is noteworthy to observe that the HG hypoxia condition shows a lot of Alcian blue staining but also exhibits the highest fibroblast-like structure score, leaving the total score negative. Upon reviewing the COL2a staining, illustrated in figure 6, discernible staining is primarily observed in the HG normoxia pellet. This COL2a staining corresponds with the Alcian Blue staining that highlights the chondrocyte-like structures. Notable, COL2a is not visible in areas where a looser pellet structure is present.

Table 1, Alcian blue pellets were assessed based on color intensity, the presence of fibroblast-like structures and the degree of centralization of the staining. We observe that HG normoxia exhibits the highest total score, indicating the most pronounced chondrocyte-like structure. Conversely HG hypoxia displays the least chondrocyte-like structure.

Day 21	Intensity Alcian blue	Fibroblast-like structure	Centered	total
HG normoxia	4,1	- 2,33	0,4	2,17
LG normoxia	2,61	- 1,77	0,15	0,99
HG hypoxia	3,28	- 3,96	0	-0,68
LG hypoxia	0,81	- 1,2	0	-0,39

H4.2 Normoxia stimulates lipogenesis

As depicted in figure 7, normoxia exhibits a higher abundance of lipid droplets, indicating a positive impact on lipogenesis. However, no discernible difference is apparent between the HG and LG conditions. To thoroughly ascertain the absence of difference in lipid droplet formation between HG and LG, we conducted a quantification, presented in table 2. This table affirms that there is no significant difference between HG and LG conditions, reinforcing that only the positive influence of normoxia is evident. Additionally, there is no visually apparent difference in the width of lipid droplets among the various conditions.

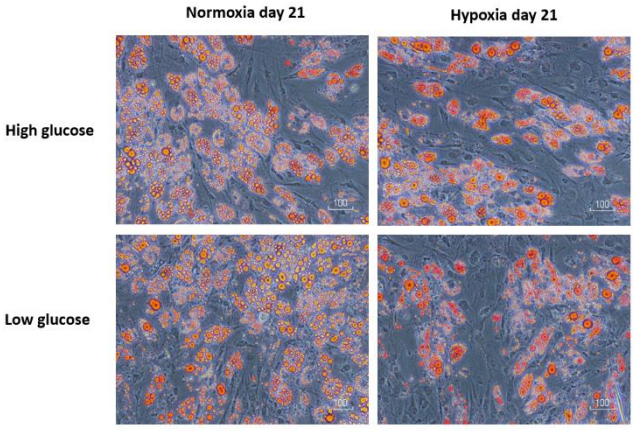

Oil red O extraction	Normoxia	Hypoxia
High glucose	0,074 ± 0,003	0,047 ± 0,006
Low glucose	0,071 ± 0,010	0,041 ± 0,005

Figure 7, (Left) Adipocytes were stained with Oil Red O, and images were acquired using a Nikon microscope (scalebar 100 µm). In normoxic conditions, a higher formation of lipid droplets is observed compared to hypoxic conditions. No visible differences are noted between HG and LG conditions and there is also no apparent distinction in the size of the lipid droplets. (Right) Quantification of Oil red O. This table concludes that normoxia shows a higher formation of lipid droplets, and that hypoxia has less lipid formation. Also this table concludes that there is no significant difference between HG and LG.

H4.3 No signs of osteogenic differentiation

The results of the alizarin red S staining, seen in figure 8, reveals the absence of any calcium deposits, indication a lack of osteogenic differentiation in our hMSCs. A closer examination of cell morphology further supports this conclusion, as the absence of calcium phosphates and the expansive cell surface collectively indicate that osteogenic differentiation has not occurred.

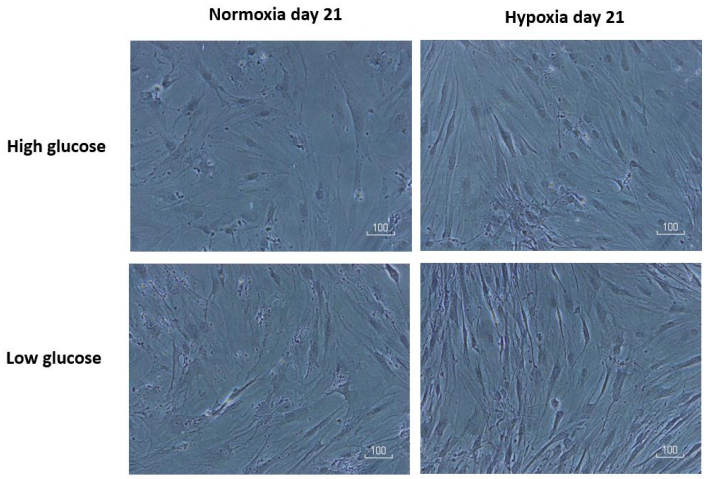

Figure 8, Alizarin red S staining, images were acquired using a Nikon microscope (scalebar 100 µm). Measurement revealed no visible staining in any of the conditions.

H5 Discussion

Upon analyzing the results, distinct outcomes emerge across the four conditions. HG normoxia demonstrates the highest degree of chondrogenic differentiation, succeeded by HG hypoxia, followed by LG normoxia and LG hypoxia displaying the least chondrogenic differentiation. This observation proves that glucose and oxygen concentrations do have an influence on the differentiation of hMSC's into chondrocytes. Besides chondrogenic differentiation, adipogenesis is also influenced by oxygen, leading to a better differentiation in normoxia conditions than in hypoxia conditions.

Reviewing the glucose metabolism we see that glucose can be converted through aerobic and anaerobic processes. The aerobic pathway, known for its superior efficiency, yields a higher energy output of 36 ATP molecules, whereas the anaerobic pathway produces only 2 ATP molecules. Consequently, the disparate outcomes witnessed in our experimental conditions may be attributed to the distinctive pathways of the glucose metabolism.

H5.1 Energy shortage leads to a lag in differentiation

When transferring the cells from the expansion flask to the well plates, trypsin is involved. Treating the cells with trypsin is a process that separates all proteins connected to the cell membrane, leading to the detachment of individual cells. Upon seeding for the differentiation experiment, cells must regenerate these lost proteins.

Under HG and normoxia conditions, cells utilize efficient energy production, enabling rapid protein synthesis and swift reestablishment of cell-to-cell contact. In contrast, LG hypoxia conditions prompt cells to employ the least favorable energy production pathway, resulting in a slower process of protein regeneration for cell-to-cell contact. This leads to the formation of fluffy and non-compact pellets, particularly evident in 3D culture, where cell aggregation and intercellular contact are crucial. This may explain the observed fluffy pellets and decrease in pellet growth over time, as the cells initially struggle to adhere to each other.

From this perspective, it is plausible that LG and hypoxia conditions necessitate more time for differentiation, implying that they are a few days to a week behind the HG normoxia pellet. This further suggest that while we have identified a condition that induces the fastest chondrogenic differentiation, we have not yet determined the optimal condition for this process.

H5.2 High glucose concentration stimulates chondrogenic differentiation

In HG conditions, where glucose is readily accessible, cells can synthesize a greater quantity of proteins. In addition to proteins facilitating cell-to-cell contact, cells can also generate proteins that specifically promote and signify differentiation. Examples of such proteins include COL2a and GAGs. As described in this study, high glucose can have a positive effect on chondrogenesis, as it synthesis GAGs and extracellular matrix. This aligns with the observed increase in pellet size, alcian blue staining and COL2a staining in HG normoxia (21).

Conversely, in the LG normoxia condition, the accessibility of glucose is limited and the cell will use the glucose molecules to either proliferate or differentiate. In this study, it was observed that when satellite cells were exposed to low glucose, the energy is utilized for proliferation, resulting in a delayed differentiation. This corresponds to the pellets in LG, where the cell density was high but less differentiation had occurred (7).

H5.3 High oxygen concentration stimulates chondrogenic differentiation

In the HG normoxia condition, cells primarily utilize the aerobic pathway to produce energy during culture. However, in hypoxia, cells undergo a shift toward anaerobic pathway. The limited availability of oxygen in hypoxia prompts a less efficient glucose breakdown, yielding only 2 ATP molecules per glucose molecule.

As a consequence, the cellular energy pool is depleted, leading to an extend duration for molecular production in hypoxic compared to normoxic conditions. This implies that hypoxia conditions will consistently lag behind the other conditions by a few days (7). This was visible by the same glucose concentration but different oxygen concentration. Whereby normoxia always showed a better (or faster) chondrogenic differentiation than hypoxia.

H5.4 COL2a stains positive in chondrocyte-like structures

A noteworthy observation is the identification of loose structures along the edges of the pellets. Even though Alcian Blue stained these areas blue. IHC staining for COL2a reveals an absence of COL2a production in these regions indicating that the cells and matrix in this particular area lack chondrogenic features. The lack of COL2a further may suggests a presence of hypertrophic chondrocytes due to the fact that there is no COL2a present in hypertrophic chondrocytes (22). Potentially leading to chondrocyte ossification. Despite HG normoxia demonstrating the most chondrocyte-like structures, it also exhibits loose fibroblast-like structures which may be signs of a hypertrophic state in the pellet. However, HG hypoxia conditions display more loose structures and less COL2a than the normoxia condition. This discrepancy requires further investigation, as it contradicts existing literature which indicates that hypoxic conditions inhibit the hypertrophic process which was mentioned in the introduction.

Besides the influence of hypoxia on the hypertrophic state of the chondrocytes, the glucose concentration also plays an important role. Due to HG, COL2a is downregulated and COL1a is upregulated (3). This may provide justification for the lack of COL2a detection at the edges of the pellets. In the center of the pellet, COL2a was demonstrated in HG normoxia pellets, possible because glucose availability in the center is less compared to the edges of the pellet.

H5.5 Hypoxia reduces lipogenesis in adipocytes

Hypoxia leads to a reduction in lipogenesis in adipocytes, aligning with the expected outcome and literature findings. The stimulation of HIF1a results in decreased lipogenesis, leading to fewer lipid droplets. The observed results align with literature references (4, 23).

Surprisingly, no significant difference was measured between HG and LG. This implies that glucose has minimal influence on lipid droplet formation. This result contradicts existing literature, as studies suggest that a high glucose concentration should stimulate adipogenesis. The literature indicates that high glucose should lead to an increase in PPAR-gamma, adiponectin and lipoprotein lipase, ultimately promoting adipogenesis (24, 25). This deviation from literature warrants further investigation.

H5.6 Donors are not able to differentiate into osteocytes

The donors used were not subjected to osteogenic differentiation. Given the utilization of a standard protocol condition, which also exhibited no differentiation, we assume that the issue does not lie with the differentiation media. In this study, the same donors were used, where by also a lack of effective differentiation was observed (34).

H6 Conclusion

In this study, we hypothesized that low glucose concentration in a hypoxic environment would induce optimal chondrogenic differentiation. However, our results indicate that low glucose in hypoxic conditions does not lead to the fastest differentiation. Instead high glucose in normoxic conditions demonstrates accelerated cell compaction in 3D cell culture, subsequently promoting quicker differentiation into chondrocytes. Due to uncertainty regarding whether other conditions were merely slower than high glucose normoxia, we cannot definitively assert that high glucose normoxia is the superior condition.

Furthermore, our prediction regarding the impact of hypoxia on lipogenesis holds true, as normoxia exhibits increased lipid droplets and higher absorbance. This suggest that adipocytes thrive better in normoxia. No significant difference were observed between high and low glucose in both normoxia and hypoxia conditions, concluding that there is not a big influence of glucose on the differentiation.

Lastly, our findings indicate a limited differential potential of the utilized hMSCs into osteocytes, precluding us from drawing conclusions regarding the optimal condition for osteogenic differentiation.

H7 Recommendations

As this is an interesting start of investigating what the influence of glucose and oxygen is on the differentiation of hMSCs, futher research is needed.

H7.1 Culturing for more than 21 days

When examining our results, it appears that the low glucose and low oxygen concentration conditions may lag behind by a few days. To ascertain whether differentiation occurs later in this condition, extending the experiments duration from 21 days to 28 or 35 days would be of interest. This extension could provide insight into whether differentiation indeed takes a longer period or if the conditions simply does not promote differentiation. Ultimately, this approach will yield a more robust answer regarding the optimal condition for hMSCs differentiation.

H7.2 IHC on hypertrophic proteins

To elucidate the prevalence of fibroblast-like structures in the pellets, it is of interest to assess the pellets for hypertrophic proteins. Given the absence of COL2a proteins in these regions of the pellets, it implies that they do not represent as “typical” chondrocytes. Hypertrophic chondrocytes also lack COL2a in the matrix, suggesting that the cells might exhibit hypertrophic characteristics. This hypothesis can be tested through IHC targeting specific hypertrophic proteins such as COL10a or MMP13 (22).

H7.3 Different concentrations of glucose

We have observed that high glucose is favorable for chondrogenic differentiation, but the optimal concentration for differentiation remains uncertain. It is possible that the pellets might exhibit improved differentiation within a glucose concentration ranging between 1 and 4.5 g/L. Therefore, investigating the influence of various glucose concentration becomes of interest. It is worth considering the potential impact of slower differentiation at lower glucose concentration and conducting tests for hypertrophic properties of the pellets in these conditions as well.

References

1. Studer D, Millan C, Öztürk E, Maniura-Weber K, Zenobi-Wong M. Molecular and biophysical mechanisms regulating hypertrophic differentiation in chondrocytes and mesenchymal stem cells. Eur Cell Mater. 2012;24:118-35; discussion 35.
2. Sun C, Lan W, Li B, Zuo R, Xing H, Liu M, et al. Glucose regulates tissue-specific chondro-osteogenic differentiation of human cartilage endplate stem cells via O-GlcNAcylation of Sox9 and Runx2. Stem Cell Res Ther. 2019;10(1):357.
3. Sun C, Shang J, Yao Y, Yin X, Liu M, Liu H, et al. O-GlcNAcylation: a bridge between glucose and cell differentiation. J Cell Mol Med. 2016;20(5):769-81.
4. Trayhurn P, Alomar SY. Oxygen Deprivation and the Cellular Response to Hypoxia in Adipocytes – Perspectives on White and Brown Adipose Tissues in Obesity. Frontiers in Endocrinology. 2015;6.
5. Kolios G, Moodley Y. Introduction to stem cells and regenerative medicine. Respiration. 2013;85(1):3-10.
6. Vater C, Kasten P, Stiehler M. Culture media for the differentiation of mesenchymal stromal cells. Acta Biomaterialia. 2011;7(2):463-77.
7. Furuichi Y, Kawabata Y, Aoki M, Mita Y, Fujii NL, Manabe Y. Excess Glucose Impedes the Proliferation of Skeletal Muscle Satellite Cells Under Adherent Culture Conditions. Front Cell Dev Biol. 2021;9:640399.
8. Mas-Bargues C, Sanz-Ros J, Román-Domínguez A, Inglés M, Gimeno-Mallench L, El Alami M, et al. Relevance of Oxygen Concentration in Stem Cell Culture for Regenerative Medicine. Int J Mol Sci. 2019;20(5).
9. Brown GK. Glucose transporters: structure, function and consequences of deficiency. J Inherit Metab Dis. 2000;23(3):237-46.
10. Lu S, Sun X, Zhang Y. Insight into metabolism of CHO cells at low glucose concentration on the basis of the determination of intracellular metabolites. Process Biochemistry. 2005;40(5):1917-21.
11. Akram M. Citric Acid Cycle and Role of its Intermediates in Metabolism. Cell Biochemistry and Biophysics. 2014;68(3):475-8.
12. Tsai TL, Manner PA, Li WJ. Regulation of mesenchymal stem cell chondrogenesis by glucose through protein kinase C/transforming growth factor signaling. Osteoarthritis and Cartilage. 2013;21(2):368-76.
13. Morita K, Miyamoto T, Fujita N, Kubota Y, Ito K, Takubo K, et al. Reactive oxygen species induce chondrocyte hypertrophy in endochondral ossification. Journal of Experimental Medicine. 2007;204(7):1613-23.
14. Leijten J, Georgi N, Moreira Teixeira L, van Blitterswijk CA, Post JN, Karperien M. Metabolic programming of mesenchymal stromal cells by oxygen tension directs chondrogenic cell fate. Proceedings of the National Academy of Sciences. 2014;111(38):13954-9.
15. Chuang CC, Yang RS, Tsai KS, Ho FM, Liu SH. Hyperglycemia Enhances Adipogenic Induction of Lipid Accumulation: Involvement of Extracellular Signal-Regulated Protein Kinase 1/2, Phosphoinositide 3-Kinase/Akt, and Peroxisome Proliferator-Activated Receptor γ Signaling. Endocrinology. 2007;148(9):4267-75.
16. Kim KH, Song MJ, Chung J, Park H, Kim JB. Hypoxia inhibits adipocyte differentiation in a HDAC-independent manner. Biochem Biophys Res Commun. 2005;333(4):1178-84.
17. Li Y-M, Schilling T, Benisch P, Zeck S, Meissner-Weigl J, Schneider D, et al. Effects of high glucose on mesenchymal stem cell proliferation and differentiation. Biochemical and Biophysical Research Communications. 2007;363(1):209-15.
18. Liu Z, Jiang H, Dong K, Liu S, Zhou W, Zhang J, et al. Different Concentrations of Glucose Regulate Proliferation and Osteogenic Differentiation of Osteoblasts Via the PI3 Kinase/Akt Pathway. Implant Dentistry. 2015;24(1).
19. Yao Y, Deng Q, Song W, Zhang H, Li Y, Yang Y, et al. MIF Plays a Key Role in Regulating Tissue-Specific Chondro-Osteogenic Differentiation Fate of Human Cartilage Endplate Stem Cells under Hypoxia. Stem Cell Reports. 2016;7(2):249-62.
20. Boskey AL. Signaling in response to hypoxia and normoxia in the intervertebral disc. Arthritis Rheum. 2008;58(12):3637-9.
21. Han Y-S, Bang O-S, Jin E-J, Park J-H, Sonn J-K, Kang S-S. High dose of glucose promotes chondrogenesis via PKCα and MAPK signaling pathways in chick mesenchymal cells. Cell and Tissue Research. 2004;318(3):571-8.
22. Green JD, Tollemar V, Dougherty M, Yan Z, Yin L, Ye J, et al. Multifaceted signaling regulators of chondrogenesis: Implications in cartilage regeneration and tissue engineering. Genes & Diseases. 2015;2(4):307-27.

23. Zhou S, Lechpammer S, Greenberger JS, Glowacki J. Hypoxia inhibition of adipocytogenesis in human bone marrow stromal cells requires transforming growth factor-beta/Smad3 signaling. J Biol Chem. 2005;280(24):22688-96.
24. Aguiari P, Leo S, Zavan B, Vindigni V, Rimessi A, Bianchi K, et al. High glucose induces adipogenic differentiation of muscle-derived stem cells. Proceedings of the National Academy of Sciences. 2008;105(4):1226-31.
25. Jackson RM, Griesel BA, Gurley JM, Szweda LI, Olson AL. Glucose availability controls adipogenesis in mouse 3T3-L1 adipocytes via up-regulation of nicotinamide metabolism. Journal of Biological Chemistry. 2017;292(45):18556-64.
26. Scott JE, Quintarelli G, Dellovo MC. The chemical and histochemical properties of Alcian Blue. I. The mechanism of Alcian Blue staining. Histochemie. 1964;4(2):73-85.
27. Mehlem A, Hagberg CE, Muhl L, Eriksson U, Falkevall A. Imaging of neutral lipids by oil red O for analyzing the metabolic status in health and disease. Nature Protocols. 2013;8(6):1149-54.
28. Moriguchi T, Yano K, Nakagawa S, Kaji F. Elucidation of adsorption mechanism of bone-staining agent alizarin red S on hydroxyapatite by FT-IR microspectroscopy. Journal of Colloid and Interface Science. 2003;260(1):19-25.
29. Churukian CJ. 14 - Pigments and Minerals. In: Bancroft JD, Gamble M, editors. Theory and Practice of Histological Techniques (Sixth Edition). Edinburgh: Churchill Livingstone; 2008. p. 233-59.
30. Magaki S, Hojat SA, Wei B, So A, Yong WH. An Introduction to the Performance of Immunohistochemistry. Methods Mol Biol. 2019;1897:289-98.
31. Lian C, Wang X, Qiu X, Wu Z, Gao B, Liu L, et al. Collagen type II suppresses articular chondrocyte hypertrophy and osteoarthritis progression by promoting integrin β1−SMAD1 interaction. Bone Research. 2019;7(1):8.
32. Nazaret C, Heiske M, Thurley K, Mazat J-P. Mitochondrial energetic metabolism: A simplified model of TCA cycle with ATP production. Journal of Theoretical Biology. 2009;258(3):455-64.
33. Czibik G, Steeples V, Yavari A, Ashrafian H. Citric acid cycle intermediates in cardioprotection. Circ Cardiovasc Genet. 2014;7(5):711-9.
34. Georgi N. Epigenetic changes associate with improved performance of MSC's expanded in hypoxia. Multiple Choice: Leveraging instructive culture models to improve cartilage tissue engineering. 2013.
35. Bonsib S, Bhalodia A, Haque A, et al. Special Stains and H & E Second Edition. chrome-extension://efaidnbmnnnibpcajpcglclefindmkaj/https://www.agilent.com/cs/library/technicaloverviews/public/08066_special_stains_eduguide.pdf
36. Sigmaaldrich. Alcian blue staining kit, pH 1.0. https://www.sigmaaldrich.com/NL/en/product/mm/132647.
37. Sigmaaldrich. Oil red O. https://www.sigmaaldrich.com/NL/en/product/sial/o0625?icid=sharepdp-clipboard-copy-productdetailpage

Appendix

A Cytochemical staining

B1 Alcian blue

Alcian Blue is a mostly used cationic dye and can be used to identify chondrocytes (35). The Alcian Blue molecule has a copper-containing phthalocyanine ring structure with three to four isothiouronium groups, which give the molecule a positive charge. Starting from the copper-containing phthalocyanine ring structure, the molecule undergoes two reaction steps to form a Alcian Blue molecule seen in figure 11:

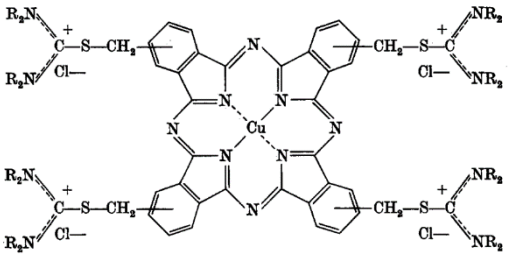

Figure 3, Structure of Alcian Blue molecule (36).

1) $Cu\ Phthalocyanine \xrightarrow{chloromethylation} Cu\ Phthalocyanine - (CH_2\ Cl)_x$

2) $Cu\ Phthalocyanine - (CH_2\ Cl)_x \xrightarrow{substituted\ thioures} Cu\ Phthalocyanine - (CH_2 - S - C - (NR_2)_2)_y$

The Copper-containing phthalocyanine is the chromophore of the molecule and gives the molecule the blue color (26). The isothiouronium are the cationic groups that will carry the molecule to a polyanion, such as sulfated glycosaminoglycans (GAGs). GAGs are negatively charged polysaccharide compounds that will attract to the Alcian Blue molecule by coulombic attraction. This attraction will lead to the formation of an ionic bond. When Alcian blue is linked to a polyanion, the dye will not be washed away and the polyanion appears blue. Because Alcian blue can bind to several polyanions, it is not a specific dye. This means it can also dye unsuspected presences of acid groups. This needs to be taken into account when seeing unexpected staining (26). Alcian Blue is mostly kept in a low pH, such as 1 or 2.5. This makes sure the carboxyl group of the Alcian Blue molecule will not be dissociated. The lower the pH the more strongly sulfated polyanions it will stain (35). The counter stain of Alcian Blue is nuclear fast red, which is a acidic compound that will dye the cell nuclei dark red and the cytoplasm light red.

B2 Oil red O

Oil red O is a lysochrome that can detect neutral triglycerides and lipids on frozen sections and lipoproteins on paraffin sections. It is a fat-soluble diazol dye and is used to stain fat in tissue, seen in figure 12. The staining is a supersaturated solutions of Oil red O in isopropanol. The histological mechanism of staining lipids relies on the dye's physical properties, where it is minimally soluble in the solvent. Due to the hydrophobic preference the dye will therefore migrate from the solvent to the lipids. After staining, the dye can be extracted using 4% v/v Nonidet P-40 and then quantified by measuring the absorbance at 518 nm (27).

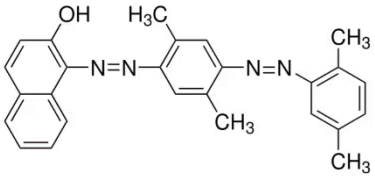

Figure 4, Structure of Oil red O molecule (37).

B3 Alizarin red S

Alizarin red S is used to detect calcium deposits in tissue. Alizarin red S is water-soluble and contains a sodium atom, two hydroxyl groups and two double bonded oxygens, see figure 13 (28). The two hydroxyl groups have a strong affinity for the insoluble and inorganic calcium salts in tissue. This can lead to a reaction between the two molecules, whereby Alizarin red S is bound to calcium leaving a stable complex. This complex precipitates in tissue, creating a red visible color. Alizarin red S is a pH dependent. The binding characteristics change due to the acidic conditions in which Alizarin red S reacts. Research has found an optimum binding of Alizarin red S with calcium at a pH of 4.2, whereby it specifically stains calcium ions (29).

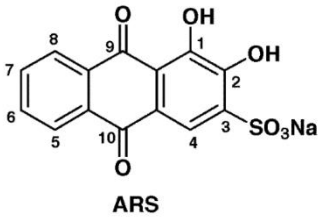

Figure 5, Structure of Alizarin red S.

B Immunohistochemical staining

C1 COL2A

Another way to analyze cells is immunohistochemistry (IHC). IHC is a widely used testing method to classify the cell type. This method is based on marking antigens that specify a specific cell type. It is most commonly used on formalin fixed paraffin embedded (FFPE) tissue and is based on the chemistry of an antigen-antibody reaction. One of the first steps of IHC is antigen retrieval. This step includes the pretreatment of the cells and make the tissue more accessible to antibody binding. This step helps increase the sensitivity of the IHC staining. Next, the sample is exposed to a primary antibody to heighten the contrast between positively stained tissue and any non-specific background staining. Subsequently, a second antibody is introduced to the sample, binding to the primary antigens. This labeled secondary antibody then magnifies the signal. To observe the antigen/antibody interaction, a chromogen is applied, resulting in a colored product after incubation with the tissue sample (30).

For chondrocytes, COL2a1 can be used as a primary antigen. COL2a1 is a major component of the cartilage matrix. It can regulate cell proliferation, metabolism and cell differentiation of chondrocytes. It is a very specific antigen to classify a chondrocyte (31).

C Citric acid cycle (CTA)

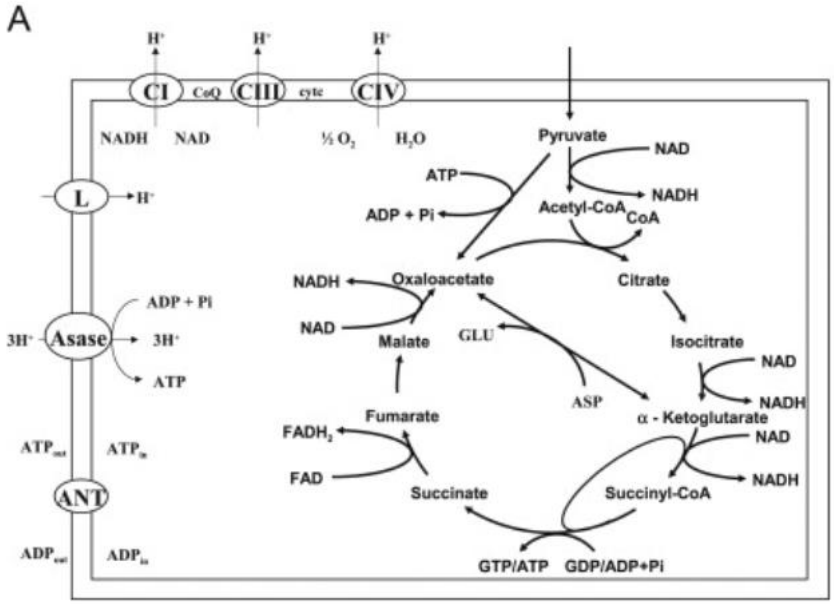

Figure 6, Citric acid cycle molecular metabolism (32).

Glucose undergoes conversion to acetyl-CoA (2C) and subsequently combines with oxaloacetate (4C) to yield a citrate (6C) molecule. This reaction is catalyzed by the enzyme citrate synthase. Following this, citrate undergoes isomerization to isocitrate (6C) by the enzyme aconitase. Isocitrate is further metabolized via oxidation by isocitrate dehydrogenase, resulting in the production of alpha-ketoglutarate (5C), accompanied by the generation of one NADH and one CO_2 molecule. The alpha-ketoglutarate generated is then enzymatically transformed into succinyl-CoA (4C) by alpha-ketoglutarate dehydrogenase, leading to the production of another NADH and CO_2 molecule. Succinyl-CoA is subsequently converted into succinate via succinyl-CoA synthase, yielding one GTP molecule. The ensuing conversion of succinate into fumarate, facilitated by succinate dehydrogenase, yield one QH_2 and serves as a substrate for $FADH_2$ production. Fumarate undergoes conversion into malate, mediated by the enzyme fumarase, and this process concludes with the conversion of malate into oxaloacetate through malate dehydrogenase, generating one

NADH. Oxaloacetate, in turn, initiates a new cycle of the tricarboxylic acid cycle (TCA). Due to the fact that one glucose molecule is converted into two acetyl-CoA molecules, this process delivers 6 NADH molecules, 2 $FADH_2$ molecule, 2 GTP molecule and 4 CO_2 molecules (11, 33). For the molecular metabolism of the TCA, see figure 1.

Within the mitochondria, two membranes exist: the outer membrane and the inner membrane.. Notably, the inner membrane exhibits impermeability to ions. Molecules acquired, such as NADH, $FADH_2$, GTP and CO_2, are capable of donating electrons to enzyme complexes such as complex I and complex II. These complexes utilize these electrons to actively transport protons (H^+) into the intermembrane space, thereby establishing an electrochemical gradient. As a consequence of this gradient, protons undergo transportation back into the matrix via ATP synthase, facilitating the conversion of ADP and phosphate into ATP. This process constitutes the synthesis of ATP, a pivotal energy-carrying molecule. Giving a net total of 36 ATP molecules (32, 33)

D Pellet width over time

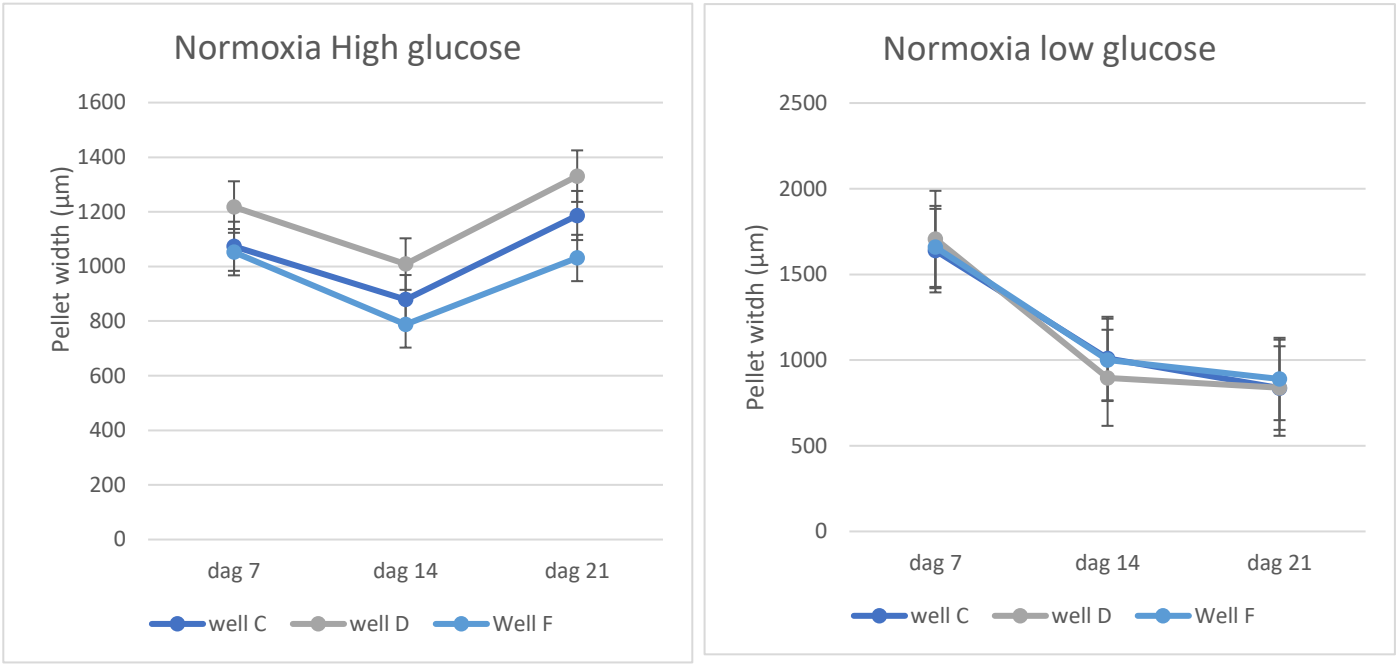

Figure 7, Graph of pellet width over time of HG and LG normoxic conditions. This figure shows that both conditions first undergo a shrinkage but after day 14 HG increases in size and LG still decreases a little bit.

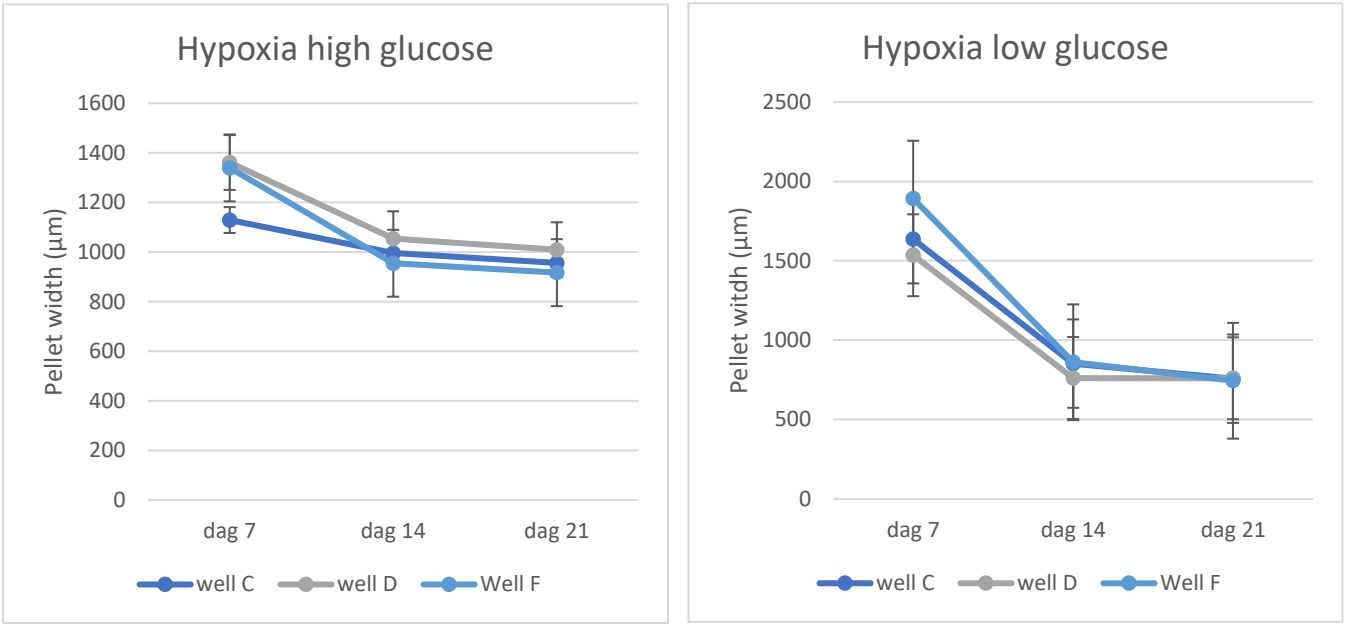

Figure 9, Graph of pellet width over time of HG and LG hypoxic conditions. In this graph it is also visible that both conditions undergo the most shrinkage between day 7 and day 14. After day 14, the pellets still decrease a little bit but not as much as before.

E Oil red O extraction measurement

Abs	1	2	3	4	5	6	7	8	9	10	11	12
A	Nor HG well A1	Nor HG well A2	Nor HG well A3	or LG well B1	Nor LG well B2	Nor LG well B3	Hyp HG well A1	yp HG well A2	Hyp HG well A3	lyp LG well B1	Hyp LG well B2	Hyp LG well B3
B	Nor HG well A1	Nor HG well A2	Nor HG well A3	or LG well B1	Nor LG well B2	Nor LG well B3	Hyp HG well A1	o HG well CA2	Hyp HG well A3	lyp LG well B1	Hyp LG well B2	Hyp LG well B3
C	Nor HG well A1	Nor HG well A2	Nor HG well A3	or LG well B1	Nor LG well B2	Nor LG well B3	Hyp HG well A1	yp HG well A2	Hyp HG well A3	lyp LG well B1	Hyp LG well B2	Hyp LG well B3
D												
E	Blanco											
F	Blanco											
G	Blanco											
H												

Figure 8, A schematic representation of the microtiter plate, illustrating its layout, is presented above. Every color means a culture condition. Every different intensity in color means a different well in the same culture conditions.

Abs	1	2	3	4	5	6	7	8	9	10	11	12
A	0,1159	0,1111	0,1165	0,1242	0,1113	0,1019	0,0956	0,0820	0,0852	0,0889	0,0835	0,0775
B	0,1113	0,1090	0,1139	0,1207	0,1096	0,0975	0,0928	0,0797	0,0846	0,0748	0,0820	0,0759
C	0,1145	0,1081	0,1128	0,1200	0,1083	0,0991	0,0941	0,0799	0,0833	0,0747	0,0833	0,0762
D	0,0485	0,0484	0,0478	0,0481	0,0481	0,0477	0,0478	0,0480	0,0480	0,0479	0,0478	0,0479
E	0,0399	0,0501	0,0480	0,0481	0,0481	0,0478	0,0480	0,0485	0,0484	0,0485	0,0478	0,0482
F	0,0386	0,0483	0,0483	0,0483	0,0480	0,0481	0,0478	0,0484	0,0478	0,0485	0,0478	0,0479
G	0,0387	0,0481	0,0480	0,0480	0,0480	0,0479	0,0481	0,0479	0,0479	0,0478	0,0478	0,0477
H	0,0483	0,0489	0,0488	0,0494	0,0488	0,0482	0,0483	0,0483	0,0480	0,0484	0,0480	0,0487

Figure 9, The results of the Oil Red O extraction measurement indicate the extraction values under different conditions, with the plate layout specified in figure 7. Every color means a culture condition. Every different intensity in color means a different well in the same culture conditions.

Figure 7, showing oil red o extraction measurement. HG displaying the most chondrogenic differentiation and LG the least favorable.